

## **Supporting Information**

### **Ground State Destabilization From a Positioned General Base in the Ketosteroid Isomerase Active Site**

*Eliza A. Ruben, Jason P. Schwans, Matthew Sonnett, Aditya Natarajan, Ana Gonzalez, Yingsu Tsai, and Daniel Herschlag*

#### **Supporting Text**

Prior structural studies of pKSI and the structural studies of tKSI reported herein indicate that bound steroid ligands can occupy two conformations (59, 60). Ligands can bind in a forward conformation with the A-ring situated near the general base and the D-ring solvent exposed (a productive conformation), or in a nonproductive backward conformation with the D-ring situated near the general base and the A-ring solvent exposed. To test if the ligands used herein bind with the A-ring near the general base, as needed for the KSI isomerization reaction, we compared the binding affinities of ligands with identical A-rings, but with a hydroxyl, sulfate, or hemisuccinate substituent on the D-ring (Figure S3A). If the ligands bind with the A-ring near residue 38, the binding affinities for the 19-NT analogs would be expected to be the same, but if the ligands bind with the D-ring situated near residue 38, the binding affinities for the 19-NT analogs would be expected to differ. The results in Figure S3B show that ligands with different D-ring substituents have similar binding affinities for each Asp38 mutant. Further, each ligand shows a similar increase in binding affinity upon introduction of the Asp38Asn and Asp38Ala mutations (Tables S2 and S3). These results strongly suggest that the ligands bind with the A-ring near residue 38 in solution under our assay conditions.

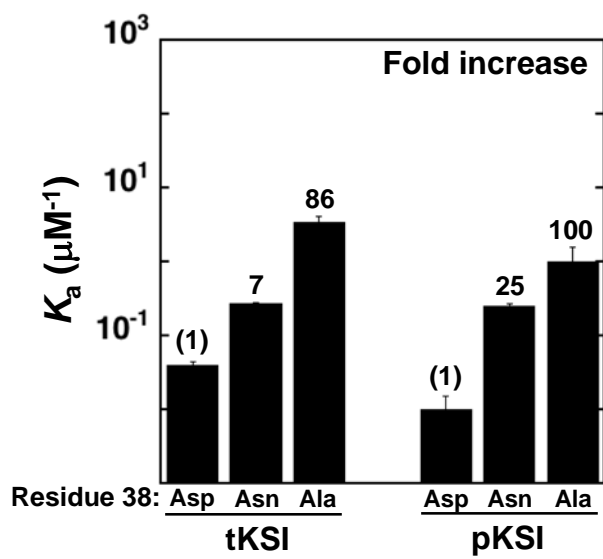


**Figure S1.** Effects of Asp38 mutations on 19-nortestosterone association constants ( $K_a$ ). Values are from Table S1.

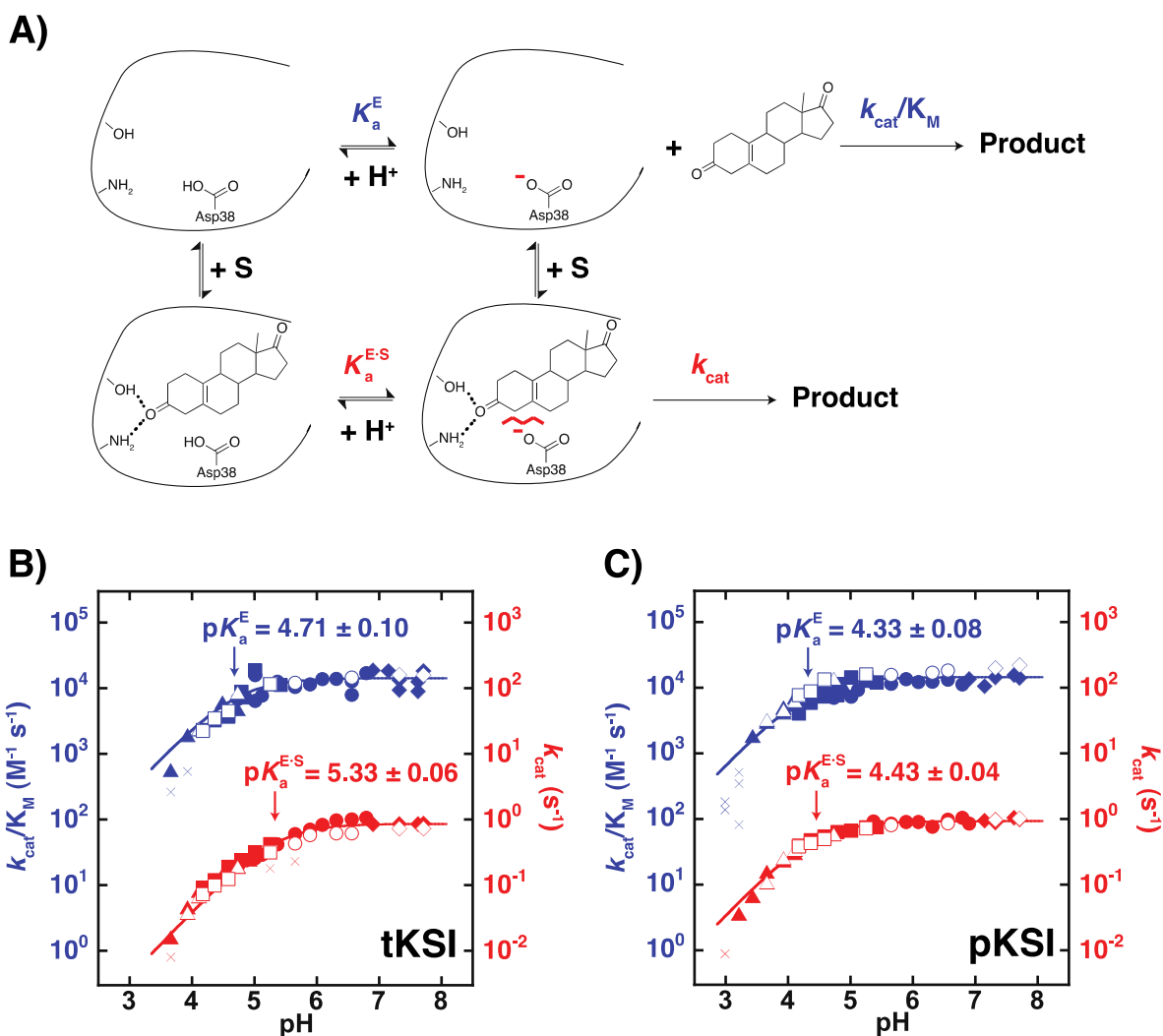


**Figure S2.** pH dependencies of  $k_{\text{cat}}/K_{\text{M}}$  and  $k_{\text{cat}}$  for tKSI and pKSI Asp99Asn with 5(10)estrene-3,17-dione. A) Reaction scheme showing that if the abutment of anionic Asp38 against bound substrate is destabilizing, the  $pK_{\text{a}}$  of the enzyme-substrate complex (E·S) is predicted to be higher than the  $pK_{\text{a}}$  of free enzyme (E). B, C) Determinations of  $k_{\text{cat}}/K_{\text{M}}$  (blue) and  $k_{\text{cat}}$  (red) for tKSI (B) and pKSI (C) Asp99Asn. Data were collected and analyzed as described in Experimental Procedures. The  $pK_{\text{a}}$  value from each fit (to a single titration) is depicted next to each titration curve with the standard error from regression analysis. Open and closed symbols represent substrate concentrations of 2.5  $\mu\text{M}$  and 5  $\mu\text{M}$  used to determine  $k_{\text{cat}}/K_{\text{M}}$ , and 300  $\mu\text{M}$  and 600  $\mu\text{M}$  used to determine  $k_{\text{cat}}$  respectively. Prior work establishes  $K_{\text{M}}$  values of 20-50  $\mu\text{M}$

for these enzymes (44). Buffers used were sodium formate (triangles), sodium acetate (squares), Na•MES (circles) and Na•MOPS (diamonds). Points omitted from the fits are depicted as ×'s. Without omitting these points, the resulting  $pK_a$  values are  $4.72 \pm 0.10$  ( $k_{cat}/K_M$ ) and  $5.41 \pm 0.07$  ( $k_{cat}$ ) for tKSI, and  $4.34 \pm 0.07$  ( $k_{cat}/K_M$ ) and  $4.42 \pm 0.04$  ( $k_{cat}$ ) for pKSI, values that do not change the conclusions.

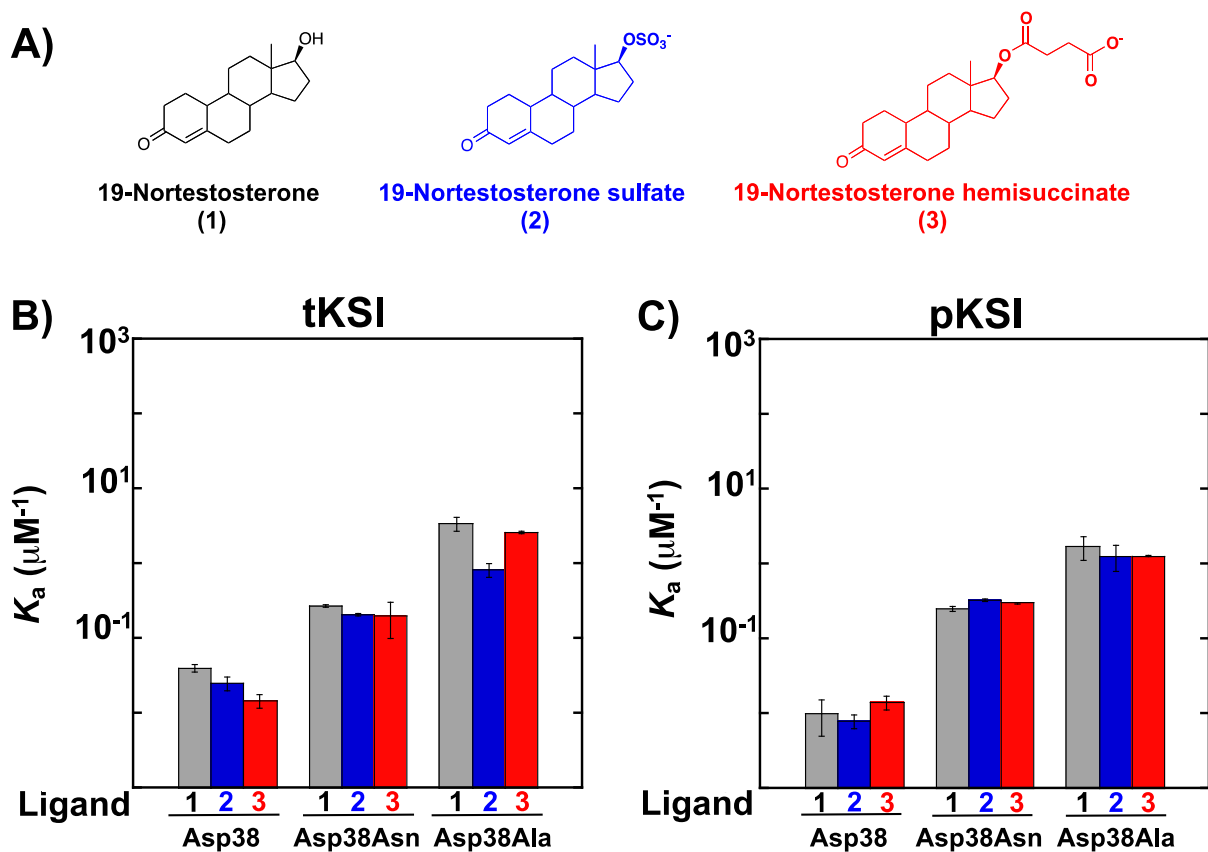


**Figure S3.** Binding affinity values with ligands having identical A-rings but different D-ring substituents. A) Structures of the ligands used in the measurements. B) Association constants for ligand binding to tKSI and pKSI. Ligands are color-coded and numbered as in panel A. Values are from Tables S2 and S3.

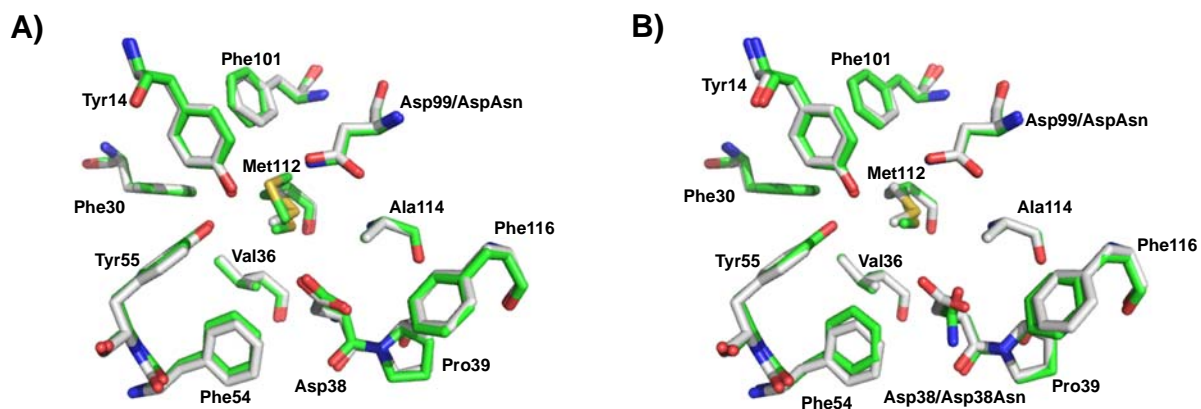


**Figure S4.** Superposition of the x-ray structures of the tKSI D99N and D38N/D99N mutants bound with 4AND with wild-type unliganded tKSI showing that the side chains surrounding residue 38 are superimposable. The (A) 1.6 Å D99N•4-AND structure (PDB ID 3NHX, carbon atoms colored green) and (B) 1.8 Å tKSI D38N/D99N•4AND structure (PDB ID 3NUV, carbon atoms colored green) both determined herein (see Table 2) each superimposed with the previously determined 2.3 Å wild type structure (PDB ID 8CHO, colored gray). The ligand is omitted for clarity. The overall root-mean-square deviation between the two structures for backbone atoms is 0.2 Å. X-ray data and refinement statistics are given in Table 2.

**Table S1. Effects of Asp38 mutations on 19-NT association constants for tKSI and pKSI**

Enzyme	tKSI		pKSI	
	$K_a$ ( $\mu\text{M}^{-1}$ )	$K_a$ ratio (Mutant/WT)	$K_a$ ( $\mu\text{M}^{-1}$ )	$K_a$ ratio (Mutant/WT)
Wild type	$(4.0 \pm 0.04) \times 10^{-2}$	[1]*	$(1.0 \pm 0.05) \times 10^{-2}$	[1]*
D38N	$(2.7 \pm 0.1) \times 10^{-1}$	7	$(2.5 \pm 0.2) \times 10^{-1}$	25
D38A	$3.4 \pm 0.7$	86	$1.0 \pm 0.6$	100

\* Defined as unity for comparison

• tKSI numbering is used throughout

**Table S2. Effects of Asp38 mutations on 19-NT, 19-NT sulfate, and 19-NT hemisuccinate association constants for tKSI**

Residue	19-NT		19-NT sulfate		19-NT hemisuccinate	
	$K_a$ ( $\mu\text{M}^{-1}$ )	$K_a$ ratio (Mutant/WT)	$K_a$ ( $\mu\text{M}^{-1}$ )	$K_a$ ratio (Mutant/WT)	$K_a$ ( $\mu\text{M}^{-1}$ )	$K_a$ ratio (Mutant/WT)
38						
Asp	$(4.0 \pm 0.04) \times 10^{-2}$	[1]*	$(2.5 \pm 0.05) \times 10^{-2}$	[1]*	$(1.5 \pm 0.03) \times 10^{-2}$	[1]*
Asn	$(2.7 \pm 0.01) \times 10^{-1}$	7	$(2.1 \pm 0.01) \times 10^{-1}$	8	$(2.0 \pm 0.1) \times 10^{-1}$	13
Ala	$3.4 \pm 0.7$	86	$(8.3 \pm 0.2) \times 10^{-1}$	32	$2.6 \pm 0.08$	180

\* Defined as unity for comparison

**Table S3. Effects of Asp38 mutations on 19-NT, 19-NT sulfate, and 19-NT hemisuccinate association constants for pKSI**

Residue	19-NT		19-NT sulfate		19-NT hemisuccinate	
	$K_a$ ( $\mu\text{M}^{-1}$ )	$K_a$ ratio (Mutant/WT)	$K_a$ ( $\mu\text{M}^{-1}$ )	$K_a$ ratio (Mutant/WT)	$K_a$ ( $\mu\text{M}^{-1}$ )	$K_a$ ratio (Mutant/WT)
38						
Asp	$(1.0 \pm 0.05) \times 10^{-2}$	[1]*	$(8.0 \pm 0.02) \times 10^{-3}$	[1]*	$(1.4 \pm 0.03) \times 10^{-2}$	[1]*
Asn	$(2.5 \pm 0.02) \times 10^{-1}$	25	$(3.3 \pm 0.09) \times 10^{-1}$	41	$(3.0 \pm 0.01) \times 10^{-1}$	21
Ala	$1.0 \pm 0.6$	100	$1.3 \pm 0.5$	160	$1.3 \pm 0.4$	91

\* Defined as unity for comparison

• tKSI numbering is used throughout

**Table S4. Residue 38 side chain•ligand distances in tKSI D38N•4AND and D38N/D99N•4AND crystal structures**

Residue 38	PDB ID	Resolution (Å)	Chain	Residue 38•ligand distance (Å)
Asp <sup>a</sup>	3NHX	1.6	A	2.73
Asn <sup>b</sup>	3NUV	1.8	A	3.16
			B	3.33
Average residue 38 side chain•ligand distance in D38N/D99N structure				3.25

<sup>a</sup>While KSI is a dimer, only one monomer chain is available in the D38N•4AND structure file.

<sup>b</sup>The electron density map showed density that allowed modeling of the ligand in a backward conformation in chain B and not in the reactive conformation in the D38N/D99N•4AND structure file.



**Table S5. Effects of Asp38 mutations on 4-AND association constants for tKSI in the Pro39Ala background**

Enzyme	$K_a$ ( $\mu\text{M}^{-1}$ )	$K_a$ ratio (Mutant/P39A)
P39A	$(2.5 \pm 0.03) \times 10^{-2}$	[1]*
D38N/P39A	$(7.4 \pm 0.2) \times 10^{-2}$	3
D38A/P39A	$(2.1 \pm 0.2) \times 10^{-1}$	8

\* Defined as unity for comparison

**Table S6. Effects of Asp38 mutations on 4-AND association constants for tKSI in the Pro39Gly background**

Enzyme	$K_a$ ( $\mu\text{M}^{-1}$ )	$K_a$ ratio (Mutant/P39G)
P39G	$(5.5 \pm 0.1) \times 10^{-2}$	[1]*
D38N/P39G	$(4.0 \pm 0.1) \times 10^{-2}$	0.7
D38A/P39G	$(6.9 \pm 0.2) \times 10^{-2}$	1.3

\* Defined as unity for comparison